SAPIENZA
UNIVERSITÀ DI ROMA

Building a template bank

Corso di Laurea Magistrale in Fisica

Corso di Laurea Magistrale in Facoltà di Scienze Matematiche Fisiche e Naturali

Candidate

Giada Caneva Santoro

ID number 1490713

Thesis Advisor

Prof. Francesco Pannarale Greco

Academic Year 2018/2019

Thesis not yet defended

Building a template bank
Master's thesis. Sapienza – University of Rome

This thesis has been typeset by LaTeX and the Sapthesis class.

Author's email: giada.greenday92@gmail.com

Fortsett å gå.

Contents

Chapter 1

Introduction

More than 100 years ago, Albert Einstein predicted the existence of gravitational waves, on the basis of his theory of general relativity. Einstein predicted that the motion of two bodies, such as planets or stars—orbit each other, could cause distortions of space-time, gravitational waves. These ripples in the fabric of space-time would spread out like the ripples in a pond when a stone is tossed in, although their amplitude would be so small that it would be nearly impossible to detect by any technology foreseen at that time. It was also predicted that objects moving in an orbit would lose energy for this reason (a consequence of the law of conservation of energy), as some energy would be given off as gravitational waves, although this would be insignificantly small in all but the most extreme cases.

Gravitational waves squeeze and stretch anything in their path as they pass by. The most powerful gravitational waves are created when objects move at very high speeds. Examples of such things are orbiting pairs of black holes and neutron stars, or massive stars blowing up at the ends of their lives. There are four categories of gravitational waves based on what generates them: continuous, compact binary inspiral, stochastic, and burst. Each category of objects generates a unique or characteristic set of signal that LIGO-Virgo's interferometers can sense, and that researchers can look for in LIGO-Virgo's data.
The interferometers are designed to detect a specified range of frequencies of gravitational waves, which means that they cannot detect objects orbiting at rates that fall outside of this range of frequencies (either too low or too high).
During the final moments of the merger of two compact objects such as neutron stars or black holes the emission of gravitational waves is at its peak. The binary loses energy, largely through gravitational waves, and as a result, the two compact objects spiral in towards each other, reaching extreme velocities at the very end of this process. In the final fraction of a second of their merger a significant amount of their mass is converted into gravitational energy, and travel outward as gravitational waves, that potentially fall within the detector's sensitive range.

However, the time they spend orbiting in that range of frequencies is typically very brief. The masses of the objects involved dictate how long they emit detectable gravitational waves. Heavy objects, like black holes, move through their final inspiral phase much more rapidly than 'lighter' objects, like neutron stars. This means that black-hole merger signals are much shorter than neutron star merger signals. For

example, the first detection of a gravitational wave signal, GW150914, coming from the a pair of merging black holes, produced a signal just two-tenths of a second long. In contrast, the first neutron star merger LIGO detected in August 2017 generated a signal over 100 seconds long. This first observation was a a remarkable accomplishment: it demonstrated both the existence of binary stellar-mass black hole systems, and the fact that such mergers could occur within the current age of the universe. It also confirmed the last remaining unproven prediction of general relativity and validated its predictions of space-time distortion in the context of large scale cosmic events. Prior to this first detection, gravitational waves had only been inferred indirectly, via their effect on the timing of pulsars in binary star systems. This event marked the beginning of a new era of gravitational-wave astronomy, which would enable observations of violent astrophysical events that were not previously possible, and potentially allow the direct observation of the birth of the universe.

Chapter 2

Gravitational Wave Detection Principles

2.1 Gravitational waves in linearized gravity

2.1.1 Weak-field metric

In 1915, Albert Einstein presented his general theory of relativity which describes how mass distorts spacetime and in turn how spacetime dictates how masses flow through it. The classical Newtonian notion of gravity ,which stated that gravity arises from an action at a distance, was replaced with a geometric interpretation of the Universe, the spacetime continuum: it can be regarded as a fabric and it can be curved by the mass of an object.
Masses moving on this curved spacetime fabric will then be perceived as gravity. In general relativity, space-time is regarded as a four-dimensional manifold with a Lorentzian metric, and gravity is a manifestation of the manifold's curvature.
The spacetime curvature is associated with the stress-energy tensor of matter fields through the Einstein's field equations:

$$G_{\mu\nu} \equiv R_{\mu\nu} - \frac{1}{2} g_{\mu\nu} R = \frac{8\pi G_N}{c^4} T_{\mu\nu} \tag{2.1}$$

Where $G_{\mu\nu}$ is the Einstein tensor, $T_{\mu\nu}$ is the stress-energy tensor of matter-fields and G_N is Newton's gravitational constant.
General relativity predicts that gravity is mediated by a new type of radiation: gravitational radiation.

In 1916 Einstein found the weak-field solutions to general relativity had wave-like solutions, gravitational waves. Gravitational waves that compose gravitational radiation are ripples in the fabric of spacetime, which periodically lengthen and shorten space, and speed up and slow down time. To study the properties of gravitational waves, it is instructive to first study them in situations where the gravitational fields are weak. In the so-called weak-field approximation, one can view the metric as the Minkowski metric with a small perturbation: it is required to expand the Einstein equations around the flat-space metric, considering as a perturbation on the space-time of special relativity. Letting $x_\mu = (t, x, y, z)$ denote

the time and space coordinates, we can write the proper distance between events x_μ and $x_\mu + dx_\mu$ as

$$ds^2 = g_{\mu\nu}dx^\mu dx^\nu \approx (\eta_{\mu\nu} + h_{\mu\nu})dx_\mu dx_\nu. \qquad \|h_{\mu\nu}\| \ll 1$$

Here $\eta_{\mu\nu} = diag(-1, 1, 1, 1)$ is the usual Minkowski metric and $h_{\mu\nu}$ represents the linearised gravitational field.
The metric perturbation is referred to as $h_{\mu\nu}$: it encapsulates gravitational waves, but contains additional, non-radiative degrees of freedom as well; $\|h_{\mu\nu}\|$ means "the magnitude of a typical non-zero component of $h_{\mu\nu}$".
The condition $\|h_{\mu\nu}\| \ll 1$ requires both the gravitational field to be weak, and in addition constrains the coordinate system to be approximately Cartesian. In linearized gravity, the smallness of the perturbation means that only terms which are linear in $h_{\mu\nu}$ are considered; higher order terms are discarded. As a consequence, indices are raised and lowered using the flat metric.
The metric perturbation $h_{\mu\nu}$ transforms as a tensor under Lorentz transformations, but not under general coordinate transformations: since the numerical values of the components of a tensor depend on the reference frame, there exists a reference frame where the linearisation of the gravitational field holds on a sufficiently large region of the spacetime.
The Einstein field equations are covariant under general coordinate transformations

$$x^\mu \to x^{\mu'}(x) \tag{2.2}$$

So that the metric transforms as

$$g_{\mu\nu} \to g_{\mu'\nu'} = x^\rho{}_{,\mu'}\, x^\sigma{}_{,\nu'}\, g_{\rho\sigma} \tag{2.3}$$

This means that one is free to choose a convenient coordinate system without altering the physical predictions of the field equations. Choosing a reference frame breaks the invariance of general relativity under coordiante trasformations but it also erases spurious degrees of freedom.
However,after choosing a frame where the field is linearised, a residual gauge symmetry remains.
Under infinitesimal coordinate transformations

$$x_\mu \to x_\mu + \xi_\mu$$

using the transformation law of the metric, to lowest order $h_{\mu\nu}$ transforms as

$$h_{\mu\nu} \to h_{\mu\nu} - \partial_\mu \xi_\nu - \partial_\nu \xi_\mu$$

Linearising the Einstein field equations

All the fundamental quantities in the field equations need to be computed in order to linearise the theory. Rather than working with the metric perturbation, changing notation and using the trace-reversed perturbation makes the computation more compact and cleaner. Defining

$$\bar{h}_{\mu\nu} = h_{\mu\nu} - \frac{1}{2}\eta_{\mu\nu}h \tag{2.4}$$

and the trace

$$h = \eta^{\mu\nu}h_{\mu\nu} \tag{2.5}$$

expressing the trace-reversed field:

$$h_{\mu\nu} = \bar{h}_{\mu\nu} + \frac{1}{2}\eta_{\mu\nu}\bar{h} \tag{2.6}$$

The Rienmann tensor constructed in linearised theory is given by

$$R^{\mu}_{\nu\rho\sigma} = \partial_\rho\Gamma^{\mu}_{\nu\sigma} - \partial_\sigma\Gamma^{\mu}_{\nu\rho} \tag{2.7}$$

$$= \frac{1}{2}(\partial_\rho\partial_\nu h^{\mu}_{\nu\rho} + \partial_\sigma\partial^\mu h^{\nu\rho} - \partial_\rho\partial^\mu h^{\nu\sigma} - \partial\ {}_\sigma\partial_\nu h^{\mu}_{\rho}) \tag{2.8}$$

From this, the Ricci tensor takes the form

$$R_{\mu\nu} = R^{\rho}_{\mu\rho\nu} = \frac{1}{2}(\partial_\rho\partial_\nu h^{\rho}_{\mu} + \partial^\rho\partial_\mu h_{\nu\rho} - \Box h_{\mu\nu} - \partial_\mu\partial_\nu h) \tag{2.9}$$

The curvature scalar is obtained contracting once more:

$$R = R^{\mu}_{\mu} = (\partial_\rho\partial^\mu h^{\rho}_{\mu} - \Box h) \tag{2.10}$$

Combining all together the Einstein tensor can be expressed as

$$G_{\mu\nu} = \frac{1}{2}(\partial_\rho\partial_\nu h^{\rho}_{\mu} + \partial^\rho\partial_\mu h_{\nu\rho} - \Box h_{\mu\nu} - \partial_\mu\partial_\nu h - \eta_{\mu\nu}\partial_\rho\partial^\sigma h^{\rho}_{\sigma} + \eta_{\mu\nu}\Box h) \tag{2.11}$$

Substituting the metric perturbation $h_{\mu\nu}$ with the $trace-reversed$ perturbation $\bar{h}_{\mu\nu}$ and expandig, the linerised Einstein equations assume the compact form:

$$\Box\bar{h}_{\mu\nu} + \eta_{\mu\nu}\partial^\rho\partial^\sigma\bar{h}_{\rho\sigma} - \partial^\rho\partial^\nu\bar{h}_{\mu\rho} - \partial^\rho\partial^\mu\bar{h}_{\nu\rho} = -\frac{16\pi G_N}{c^4}T_{\mu\nu}. \tag{2.12}$$

The linearised equations of motion are gauge-invariant, and the gauge freedom can be used to simplify the form of the field equations. In the Lorentz family of gauges, choosing the harmonic gauge $\partial_\mu h_{\mu\nu} = 0$, reduces the Einstein equations to a simple wave equation that relates the trace-reversed field to the stress energy tensor:

$$\Box\bar{h}_{\mu\nu} = (\frac{\partial^2}{\partial t^2} - \frac{\partial^2}{\partial x^2} - \frac{\partial^2}{\partial y^2} - \frac{\partial^2}{\partial z^2})\bar{h}_{\mu\nu} = -\frac{16\pi G_N}{c^4}T_{\mu\nu}. \tag{2.13}$$

By imposing the harmonic gauge one has chosen the coordinates in such a way that for a single plane wave (or a superposition of plane waves with their wave vectors pointing in the same direction), the GW polarisations are perpendicular to the direction of propagation.

The harmonic gauge gives four conditions, that reduce the 10 indipendent component of the symmetric 4x4 matrix $h_{\mu\nu}$ to six indipendent component, so

it does not fix the gauge completely, leaving 4 additional components free to be gauge-fixed. If the metric perturbation is not in the harmonic gauge, by making an infinitesimal coordinate transformation

$$\bar{h}_{\mu\nu} \to \bar{h}_{\mu'\nu'} = \bar{h}_{\mu\nu} - \xi_{\mu,\nu} - \xi_{\nu,\mu} + \eta_{\mu\nu}\xi^{\rho}_{,\rho} \tag{2.14}$$

and applying the harmonic gauge condition

$$\bar{h}^{\nu'}_{\mu'\nu',} = \bar{h}^{\nu}_{\mu\nu,} - \xi^{\nu}_{\mu,\nu} \tag{2.15}$$

Therefore any metric perturbation can be put into an harmonic gauge by making an infinitesimal coordinate transformation that satisfies

$$\bar{h}^{\nu}_{\mu\nu,} = \xi^{\nu}_{\mu,\nu} \tag{2.16}$$

This is a wave equation that always admits a solution, thus one can always achieve the harmonic gauge.
Outside the source where $T_{\mu\nu} = 0$

$$\Box\bar{h}_{\mu\nu} = 0 \tag{2.17}$$

In vacuum spacetimes which are asymptotically flat ($h_{\mu\nu} \to 0$ as $r \to 0$), along with choosing the harmonic gauge, the metric perturbation can be greatly simplified using the residual gauge freedom within the harmonic gauge class.
The transverse-traceless gauge, TT-gauge, can be obtained by choosing the components of the metric tensor $h_{\mu\nu}$, so that only the ones on the plane orthogonal to the direction of propagation (transverse) are different from zero, this results in $h_{\mu\nu}$ being traceless:

$$h^{0\mu} = 0 \quad h^{i}_{i} = 0 \quad \partial^{j}h_{ij} = 0 \tag{2.18}$$

By imposing the harmonic gauge, the 10 degrees of freedom of the symmetric matrix $h_{\mu\nu}$ have reduced to six degrees of freedom, and the residual gauge freedom, associated to the four function ξ^{μ}, has further reduced these to just two degrees of freedom, which corrispond to the two possible polarization states of the gravitational wave.
Equation (2.17) has plane wave solutions, $h^{TT}_{\mu\nu}(x) = e_{ij}(k)e^{ikx}$ with $k^{\mu} = (w/c, k)$ and $w/c = |k|$. The tensor $e_{ij}(k)$ is called the polarization tensor.

In vacuum spacetimes, a plane gravitational wave with a given wave-vector k is characterized by two functions h_{+} and $h_{\times}$, while the remaining components can be set to zero by choosing the transverse-traceless gauge.
Choosing n along the z axis:

$$h^{TT}_{\mu\nu} = \begin{bmatrix} 0 & 0 & 0 & 0 \\ 0 & h_{+} & h_{\times} & 0 \\ 0 & h_{\times} & -h_{+} & 0 \\ 0 & 0 & 0 & 0 \end{bmatrix} cos[w(t - z/c)] \tag{2.19}$$

Geodesic equation and geodesic deviation

The usual notion of "gravitational force" disappears in general relativity, replaced instead by the idea that freely falling bodies follow geodesics in spacetime. Geodesics are the curved-space equivalents of straight lines, which can be found by parallel transporting the tangent vector of a curve. Given a spacetime metric $g_{\mu\nu}$ and a set of spacetime coordinates x^μ, geodesic trajectories are given by the equation:

$$\frac{d^2x^\mu}{d\tau^2} + \Gamma^\mu_{\nu\rho}(x)\frac{dx^\nu}{d\tau}\frac{dx^\rho}{d\tau} = 0 \qquad m \neq 0 \tag{2.20}$$

$$\frac{d^2x^\mu}{d\lambda^2} + \Gamma^\mu_{\nu\rho}(x)\frac{dx^\nu}{d\lambda}\frac{dx^\rho}{d\lambda} = 0 \qquad m = 0 \tag{2.21}$$

which is the classical equation of motion of a test mass in the curved background described by the metric $g_{\mu\nu}$, in the absence of external non gravitational force and where m is the mass of the object, τ represents the proper time given by $d\tau^2 = -ds^2$, and λ is some affine parameter on the geodesic. In a flat spacetime, two straight lines that are initially parallel to each other will remain parallel.
In a curved spacetime, geodesics do not satisfy this property. Instead, two nearby geodesics, separeted by ζ^μ, follow the geodesic deviation equation

$$\frac{D^2\zeta^\mu}{D\tau^2} = -R^\mu_{\nu\rho\sigma}\zeta^\rho\frac{dx^\nu}{d\tau}\frac{dx^\sigma}{d\tau} \tag{2.22}$$

where $D/D\tau$ is defined as

$$\frac{DV^\mu}{D\tau} \equiv \frac{dV^\mu}{d\tau} + \Gamma^\mu_{\nu\rho}V^\nu\frac{dx^\rho}{d\tau} \tag{2.23}$$

and denotes the covariant derivative along a curve that is parameterised by τ. The geodesic deviation equation describes the change in separation ζ^μ between two nearby geodesic. As the Rienmann tensor describes the tidal forces caused by the gravitational field, the geodesic deviation equation shows that these tidal forces can be considered as deviations of nearby geodesics.

2.1.2 Interaction of Gravitational waves with test masses

To understand how gravitational waves interact with the detectors, mirrors in the case of the interferometric detectors, it's necessary to use the geodesic equation and the geodesic deviation equation, which are also important tools for understanding the physical meaning of a given gauge choice.
In fact the physics must be invariant under coordinate trasformations but GWs and the detector description's depend on the chosen reference frame.

Transverse-traceless gauge

Gravitational waves take a particularly simple form in the TT-gauge and choosing a gauge is equivalent to selecting a reference frame. Consider a test mass initially at rest at $\tau = 0$. The geodesic equation then becomes

$$\frac{dx^i}{d\tau^2} = -[\Gamma^i_{\nu\rho}\frac{dx^\nu}{d\tau}\frac{dx^\rho}{d\tau}]_{\tau=0} = -[\Gamma^i_{00}(\frac{dx^0}{d\tau})^2]_{\tau=0} \tag{2.24}$$

by assumption

$$\frac{dx^i}{d\tau} = 0 \qquad\qquad at \quad \tau = 0 \tag{2.25}$$

since the mass is initially at rest. Expanding to first order in $h_{\mu\nu}$, the Christoffel symbol Γ^i_{00} vanishes in the TT gauge

$$\Gamma^i_{00} = \frac{1}{2}(2\partial_0 h_{0i} - \partial_i h_{00}) \tag{2.26}$$

because both h_{00} and h_{0i} are set to zero by the gauge condition. Therefore, if at time $\tau = 0$, $dx^i/d\tau$ is zero, remains zero at all times, because its derivatives also vanishes.
This shows that if two test masses are initially separated by a coordinate separation of x^i in the TT frame, and are at rest with respect to each other, they will remain at this separation.
Overall, it seems that a GW has no influence on the geodesic or on the deviation of geodesics. In other words, in the TT gauge the coordinate location of a slowly moving, freely falling body is unaffected by the GW because the coordinates move with the waves. The TT gauge illustrates that, in general relativity, the physical effects are not expressed by what happens to the coordinates since the theory is invariant under coordinate transformations: the position of test masses doesn't change because the freedom of gauge allowed to define the coordinates in such a way that they don't change. Physical effects can instead be found monitoring proper distances, or proper times.

In fact the GWs cause the proper separation between two freely falling particles to oscillate, even if the coordinate separation is constant. Consider two spatial freely falling particles, located at $z = 0$, and separated on the x axis by a coordinate distance L_c.
Consider a GW in TT gauge that propagates down the z axis, $h^{TT}_{\mu\nu}(t, z)$. The proper distance L between the two particles in the presence of the GW is given by

$$L = \int_0^{L_c} dx\sqrt{g_{xx}} = \int_0^{L_c} dx\sqrt{1 + h^{TT}_{xx}(t, z = 0)} \tag{2.27}$$

$$\simeq \int_0^{L_c} dx[1 + \frac{1}{2}h^{TT}_{xx}(t, z = 0)] \tag{2.28}$$

$$= L_c[1 + \frac{1}{2}h^{TT}_{xx}(t, z = 0)] \tag{2.29}$$

Therefore, the proper distance expands and shrinks periodically,with a fractional length change $\delta L/L$ given by

$$\frac{\delta L}{L} \simeq \frac{1}{2}h^{TT}_{xx}(t, z = 0) \tag{2.30}$$

Even though this result is calculated in the TT gauge, it is indeed gauge indipendent; h^{TT}_{xx} acts as a strain, a fractional length change. Because the time that

light travels between the two test masses is related to the proper distance, which directly relates to the accumulated phase measured by laser interferometric GW observatories, GWs leave an imprint on the time it takes for a photon to make a round trip. Consequently, interferometers can potentially measure these imprints by measuring the length difference between their arms. The "extra" phase $\delta\phi$ (if $L \ll \lambda$ so that the metric perturbation does not change value very much during a light travel time) accumulated by a photon that travels down and back the arm of a laser interferometer in the presence of a GW is $\delta\phi = 4\pi\delta L\lambda$, where λ is the photon's wavelength and δL is the distance the end mirror moves relative to the beam splitter.

Local proper reference frame

Since positions in a lab are not marked by test particles, the TT frame is not very practical. The preferred reference frame is the proper detector frame in which the test particle is free to move because of a passing gravitational wave. The path of a test particle can then be described by Newtonian equations of motion in terms of forces. There are terms proportional to the Riemann curvature tensor from the gravitational field of the Earth but also terms from static gravitational forces, Coriolis forces, etc. In order to leave only the part proportional to the Riemann tensor, earth-based detectors look for higher frequency gravitational waves, as gravitational waves with low frequencies are comparable with slowly varying Newtonian noises. The acceleration in the z-direction due to Earth's gravity can be dealt with suspension systems allowing the test mass to act as if they were in a freely falling frame in the $x - y$ plane.

Consider a detector capable of measuring changes in the proper distance, e.g. an interferometer, with a characteristic size that is much smaller than the characteristic wavelength of the GW. In this case, one can approximate the entire detector to be in a near local Lorentz frame (freely falling frame), even in the presence of GWs. This coordinate system is defined by the requirements

$$z^i(\tau) = 0, \qquad g_{ab}(t,0) = \eta_{ab}, \qquad \Gamma^a_{bc}(t,0) = 0, \tag{2.31}$$

which imply that the metric has the form

$$ds^2 \approx -dt^2 + \delta_{ij}dx^i dx^j + O(\frac{x^i x^j}{L_B^2}) \tag{2.32}$$

where L_B^2 denotes the typical variation scale of the metric. Consider now the proper distance between the two geodesics, ζ^i, to understand how the GWs influence these two test masses the geodesic deviation equation is calculated as

$$\frac{d^2\zeta^\mu}{d\tau^2} + 2\Gamma^\mu_{\nu\rho}\frac{dx^\nu}{d\tau}\frac{dx^\rho}{d\tau} + \zeta^\sigma\Gamma^\mu_{\nu\rho,\sigma}\frac{dx^\nu}{d\tau}\frac{dx^\rho}{d\tau} = 0 \tag{2.33}$$

Assuming the two test masses are moving non-relativistically, $dx^i/d\tau$ can be neglected compared to $dx^0/d\tau$. Furthermore, the term proportional to $\Gamma^\mu_\nu\rho$ is negligible compared to other terms in a near LLF. Hence,

$$\frac{d^2\zeta^\mu}{d\tau^2} + \zeta^\sigma \Gamma^i_{00,\sigma}(\frac{dx^0}{d\tau})^2 = 0 \tag{2.34}$$

Further simplifying $\zeta^\sigma \Gamma^i_{00,\sigma} \approx \zeta^j \Gamma^i_{00,j}$

$$\frac{d^2\zeta^\mu}{d\tau^2} + \zeta^j \Gamma^i_{00,j}(\frac{dx^0}{d\tau})^2 = 0 \tag{2.35}$$

But in the LLF, $R^i_{0j0} = \Gamma^i_{00,j} - \Gamma^i_{0j,0} = \Gamma^i_{00,j}$ and therefore

$$\frac{d^2\zeta^\mu}{d\tau^2} + R^i_{0j0}\zeta^j(\frac{dx^0}{d\tau})^2 = 0 \tag{2.36}$$

Because $dx^0/d\tau \approx 1$, one can approximate $\tau \approx t$:

$$\ddot{\zeta}^j = -R^i_{0j0}\zeta^j \tag{2.37}$$

The key quantity entering into the equation, the Rienmann tensor, is gauge invariant in linearized theory, it can be evaluated in any convenient coordinate system. The expression for the Rienmann tensor in terms of the TT gauge metric perturbation h^{TT}_{ij}

$$R^i_{0j0} = R_{i0j0} = -\frac{1}{2}\ddot{h}^{TT}_{ij} \tag{2.38}$$

Substituting into the previous equation, the geodesic deviation equation in the proper detector frame takes the form

$$\ddot{\zeta}^i = \frac{1}{2}\ddot{h}^{TT}_{ij}\zeta^j \tag{2.39}$$

which can be interpreted as if the influence of a GW in a near LLF resembles a Newtonian force. In general directions, the proper distance is given by

$$s = \sqrt{L^2 + h_{ij}(t)L_iL_j} \tag{2.40}$$

where L_i denotes the spatial separation between two test masses and L the associated coordinate distance. In the given metric for the proper reference frame, the proper distance is just $|L| = \sqrt{L_iL_j}$ up to fractional errors; since the only detectors taken in consideration are those with $L \ll \lambda$, these errors are smaller than the fractional distance changes caused by the GW. Therefore $|L|$ is simply identified as the proper separation. The ideal equation for analyzing an interferometric GW detector is

$$\ddot{L}^i = \frac{1}{2}\ddot{h}^{TT}_{ij}L^j \tag{2.41}$$

Ring of test masses

The effects of gravitational waves cannot be seen in isolated bodies. This is a result of the fact that a single test mass, in a frame freely falling with it, will remain at rest. At least two test masses are required to measure the effects of gravitational waves. This is also the case when one wants to measure any curvature of spacetime.

Consider a ring of test masses in the (x, y) plane of a proper detector frame, initially at rest, centred at $z = 0$, and a GW travelling in the z-direction. This situation restricts the attention to the (x, y) plane alone, because h_{ij}^{TT} is transverse to the propagation direction, so the GW will only have influence in the plane of the test masses: the only non zero compontents of the metric perturbation are

$$h_{xx}^{TT} = -h_{yy}^{TT} = h_+ \qquad\qquad h_{xy}^{TT} = h_{yx}^{TT} = h_\times \tag{2.42}$$

where $h_+(t - z)$ and $h_\times(t - z)$ are the two polarization components, which are indipendent and can be considered separately. For the plus polarization at $z = 0$ and initial conditions $h_{ij}^{TT} = 0$ at $t = 0$:

$$h_{ab}^{TT} = \begin{bmatrix} 1 & 0 \\ 0 & -1 \end{bmatrix} h_+ \cos \omega t \tag{2.43}$$

If the displacement between geodesics is $\zeta_a(t) = (x_0 + \delta x(t), y_0 + \delta y(t))$, then of $\zeta_a(t)$ is

$$\delta\ddot{x} = -\frac{h_+}{2}(x_0 + \delta x)\omega^2 \sin \omega t \tag{2.44}$$

$$\delta\ddot{y} = \frac{h_+}{2}(y_0 + \delta y)\omega^2 \sin \omega t \tag{2.45}$$

Assuming that the perturbations are $O(h)$, and thus small compared to the unperturbed locations, δx and δy can be neglected. The integrations gives the deviations caused by the plus polarisations:

$$\delta x(t) = \frac{h_+}{2} x_0 \sin \omega t \tag{2.46}$$

$$\delta y(t) = -\frac{h_+}{2} y_0 \sin \omega t \tag{2.47}$$

Similarly, for the cross polarization at $z = 0$ and initial conditions $h_{ij}^{TT} = 0$ at $t = 0$, the situation is described by the equations

$$\delta x(t) = \frac{h_\times}{2} y_0 \sin \omega t \tag{2.48}$$

$$\delta y(t) = \frac{h_\times}{2} x_0 \sin \omega t \tag{2.49}$$

This set of equations describes the changes in the x and y components for a passing gravitational wave. The plus polarization alternately stretches and compresses the ring of test masses in the x and y directions, while the cross polarization exhibits the same behavior rotated by 45° in the x - y plane.

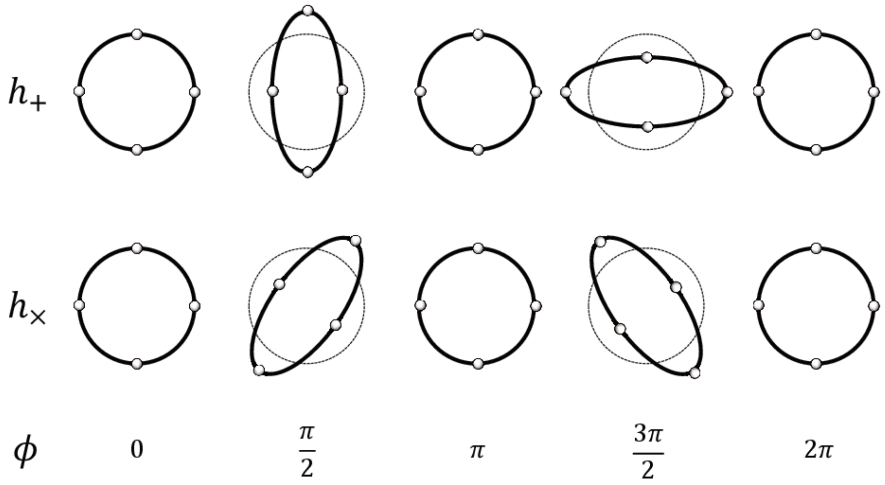

Figure 2.1. The effects of plus and cross polarization on a ring of test masses. The plus polarization alternately compresses and stretches the x- and y-separations. The cross polarization has the same effect only rotated by 45°.

2.1.3 Beam pattern functions

Interferometers are sensitive to the relative difference between two distances, the so-called strain. Suppose we have an interferometer with its arms pointing along the unit vectors u^i and v^i. The strain $h(t)$ is given by

$$h(t) = \frac{1}{2}(h_{ij}u^i u^j - h_{ij}v^i v^j) = D^{ij}h_{ij}(t) \tag{2.50}$$

where D^{ij} is referred to as the detector tensor and is given by

$$D^{ij} = \frac{1}{2}(u^i u^j - v^i v^j) \tag{2.51}$$

As the expression for $h(t)$ is linear in h_+ and $h_\times$, one can also write

$$h(t) = F_+ h_+(t) + F_\times h_\times(t) \tag{2.52}$$

where $F_{+,\times}$ are called the beam pattern functions. Suppose we have a detector with arms that are perpendicular to each other, one pointing in the x-direction and the other in the y-direction in a Cartesian coordinate system. This detector frame, denoted by (x, y, z), is generally different from the GW coordinate system, denoted by (x', y', z'), where the source is conveniently described. To account for such a difference, we first note that when the plus and cross polarisations are not equal in strength, we can rotate the coordinate system by an angle ψ around the z' axis so that the x' and y' axes coincide with the mayor and minor axis of the associated ellipse. In going from the GW frame to the detector frame, we can rotate the GW frame by an angle θ around the x' axis and an angle ϕ around the z' axis, where the angles (θ, ϕ) denote the direction of propagation of the GW in the detector frame. Applying these three rotations, the beam pattern functions for a detector with perpendicular arms are given by

$$F_{+}^{90^\circ} = \frac{1}{2}(1+\cos^2\theta)\cos 2\phi\cos 2\psi - \cos\theta\sin 2\phi\sin 2\psi \tag{2.53}$$

$$F_{\times}^{90^\circ} = \frac{1}{2}(1+\cos^2\theta)\cos 2\phi\sin 2\psi + \cos\theta\sin 2\phi\cos 2\psi \tag{2.54}$$

2.2 Gravitational Wave Interferometry

The generation and propagation of gravitational and electromagnetic radiation are basically quite similar but, on a more practical level, gravitational and electromagnetic waves are quite different. First of all, electromagnetic waves interact strongly with matter, while gravitational waves travel unperturbed through space, as they interact only very weakly with matter. This makes possible to probe astrophysics that is hidden or dark to electromagnetic observations, such as the coalescence and merger of black holes, the collapse of a stellar core, the dynamics of the early Universe. It also means that detecting gravitational waves is very difficult.
Electromagnetic radiation typically has a wavelength smaller than the size of the emitting system, and so can be used to form an image of the source, while the wavelength of gravitational radiation is typically comparable to or larger than the size of the radiating source.
Gravitational waves are generated by the bulk dynamics of the source itself so they cannot be used to form an image: the radiation simply does not resolve the generating system. In most cases, electromagnetic astronomy is based on observers obtain a large amount of information about sources on a small piece of the sky while gravitational wave astronomy is all-sky research. Detectors have nearly 4π steradian sensitivity to events over the sky. This means that any source on the sky will be detectable, not just sources towards which the detector is pointed.

Gravitational radiation is produced by oscillating multipole moments of the mass distribution of a system. Quadrupole radiation is the lowest allowed form, and is thus usually the dominant form. In this case, the gravitational wave field strength is proportional to the second time derivative of the quadrupole moment of the source, and it falls off in amplitude h, the direct observable of gravitational radiation, with distance as $1/r$. This comparatively slow fall off with radius means that relatively small improvements in the sensitivity of gravitational wave detectors can have a large impact on their science: doubling the sensitivity of a detector doubles the distance to which sources can be detected, increasing the volume of the Universe to which sources are measurable.
The oscillating quadrupolar strain pattern of a gravitational wave is well matched by a Michelson interferometer, which makes a very sensitive comparison of the lengths of its two orthogonal arms. Multiple detectors at separated sites are crucial for rejecting instrumental and environmental artifacts in the data, by requiring coincident detections in the analysis.

Also, because the antenna pattern of an interferometer is quite wide, source localisation requires triangulation using three separated detectors: the direction of travel of the GWs and the complete polarisation information carried by the waves can only be extracted by a network of detectors. The challenge is to make the instrument sufficiently sensitive: at the targeted strain sensitivity of 10^{-21} m, the

resulting arm length change is only $\tilde{1}0^{-18}$ m, a thousand times smaller than the diameter of a proton.
A key feature of the detectors is simply their scale: the arms are made as long as practically possible to increase the signal due to a gravitational wave strain.

2.2.1 Laser Interferometers

For the many decades after they were predicted, direct observation of gravitational waves was not possible due to the tiny effect that would need to be detected and separated from the background of vibrations present everywhere on Earth. A technique called interferometry was suggested in the 1960s and eventually technology developed sufficiently for this technique to become achievable.
The first gravitational wave detectors were resonant-mass cylindrical bar detectors, developed and built by Joseph Weber in the 1960s.
Over the course of the next several decades, more bar detectors were built that were at least four orders of magnitude more sensitive than Weber's original design, These detectors would be set into oscillation at their resonant frequency by passing gravitational waves near that resonant frequency and were sensitive to gravitational waves with relatively high frequency ($\sim$ 1 kHz) and in a narrow frequency band. In order to detect signals in a broader range of frequencies and out to farther distances, large-scale interferometric detectors have been built.
The idea originated with the Russian theorists, M. Gertsenshtein and V. I. Pustovoit in 1962. But the strong push for using interferometers came in the late 1960s with R. Forward, R. Weiss, R. Drever, and others. From the early 2000s, several kilometer-scale ground-based interferometers operated in the frequency band from 10 Hz to 1 kHz at a sensitivity that all owed the potential for detection from a variety of sources at large extragalactic distances.

The gravitational wave detectors are power-recycled Fabry–Perot Michelson interferometers, which offer the possibility of very high sensitivities over a wide range of frequency and are particularly suited to the detection of local perturbations in the space–time metric from astrophysical sources. These distant sources, including binary black hole or neutron star coalescences, asymmetric rapidly spinning neutron stars, and supernovae are expected to produce time-dependent strain $h(t)$ observable by the interferometer array. The optical layout of the detectors consists in perpendicular Fabry–Perot arm cavities of the Michelson, composed of mirrors, which also serve as gravitational test masses, widely separated and freely suspended as pendulums to isolate against seismic noise and reduce the effects of thermal noise. A beam splitter divides the incident laser beam into two equal components sent into the two arms of the interferometer. In each arm, a two mirrors Fabry-Perot resonant cavity extends the optical length from 3 to about 100 kilometers, because of multiple reflections and therefore increases the carrier power and phase shift for a given strain amplitude. When the beams recombine, they will interfere constructively if the lengths of the two arms differ by an integral number of wavelengths and interfere destructively if the lengths differ by an odd number of half wavelengths. The induced change in the length of the interferometer arms impresses a phase modulation on the light observed at the interferometer output, which is proportional to the wave's amplitude. Each interferometer uses a Nd:YAG laser ($\lambda = 1064nm$ or f = 282

THz). After phase modulation, the beam passes into the LIGO vacuum system. All the main interferometer optical components and beam paths are enclosed in the ultra-high vacuum system ($10^{-8} - 10^{-9} torr$) for acoustical isolation and to reduce phase fluctuations from light scattering off residual gas. The photodetectors are all located outside the vacuum system, mounted on optical tables. The beam tubes are made from stainless steel and are designed to have low-outgassing so that the required vacuum could be attained by pumping only from the ends of the tubes. The interferometer optics, including the test masses, are manufactured to have extremely low scatter and low absorption. The two Fabry-Perot arms and power recycling cavities are essential to achieving the LIGO sensitivity goal, but they require an active feedback system to maintain the interferometer at the proper operating point.

The high frequency band, $1Hz \lesssim f \lesssim 10^4 Hz$, is targeted by the new generation of ground-based laser interferometric detectors such as LIGO. The low frequency end of this band is set by the fact that it is extremely difficult to prevent mechanical coupling of the detector to ground vibrations at low frequencies, and probably impossible to prevent gravitational coupling to ground vibrations, human activity, and atmospheric motions. The high end of the band is set by the fact that it is unlikely any interesting GW source radiates at frequencies higher than a few kilohertz. Such a source would have to be relatively low mass ($\lesssim 1 M_\odot$) but extremely compact. There are no known theoretical or observational indications that gravitationally collapsed objects in this mass range exist.

2.2.2 Ground Based Interferometers

Gravitational-wave observations have become an important new means to learn about the Universe. The LIGO Scientific Collaboration and the Virgo Collaboration (LVC) have published a series of discoveries beginning with the first detected event, GW150914, a binary black hole merger. Within a span of two years, that event was followed by nine other binary black hole detections and one binary neutron star merger, GW170817. Having multiple observatories widely scattered over the globe is extremely important: the multiplicity gives rise to cross-checks that increase detection confidence and also aids in the interpretation of measurements. For example, sky location determination and concomitant measurement of the distance to a source follows from triangulation of time-of-flight differences between separated detectors.

- LIGO. The Laser Interferometer Gravitational-wave Observatory consists of three operating interferometers: a single four kilometer interferometer in Livingston, Louisiana, as well as a pair of interferometers (four kilometers and two kilometers) in the LIGO facility at Hanford, Washington. The sites are separated by roughly 3000 kilometers, and are situated to support coincidence analysis of events.

- Virgo. The Advanced Virgo detector is a Michelson laser interferometer located near Pisa, in Italy, with two orthogonal arms each 3 kilometers long. VIRGO is sensitive to gravitational waves in a wide frequency range, from 10 to 10,000 Hz.

- GEO600. GEO600 is a six hundred meter interferometer located near Hannover, Germany. It is designed and operated by scientists from the Max Planck Institute for Gravitational Physics and the Leibniz Universität Hannover. Despite its shorter arms, GEO600 achieves sensitivity comparable to the multi-kilometer instruments using advanced interferometry techniques.

- TAMA300. TAMA300 is a three hundred meter interferometer operating near Tokyo.

Non-stationary transient noise sources

The various noises of the detector can be conveniently characterized by a spectral strain sensitivity with dimensions of $1/\sqrt{Hz}$. The detector output $s(t)$ is composed of instrumental noise $n(t)$ arising from naturally occurring random processes and a potential strain signal $h(t)$

$$s(t) = n(t) + h(t) \tag{2.55}$$

The detection problem then becomes how to distinguish $h(t)$ from $n(t)$ when $h(t) << n(t)$. In a way, $n(t)$ provides a measure of how small an $h(t)$ we can detect. Thus we take $n(t)$ as the detector's noise and have a convenient way to compare performances of different detectors. The instrument response $s(t)$ can be also expressed as a convolution of the antenna patterns with the two gravitational wave polarizations $h_+, h_\times(t)$:

$$s(t) = n(t) + F_+ h_+(t) + F_\times h_\times(t) \tag{2.56}$$

The antenna patterns depend on the frequency and sky location of the source; for wavelengths that are large compared to the detector, the antenna patterns are simple quadrupoles. The information contained in the time series is usually represented in the Fourier domain as a strain amplitude spectral density, $h(f)$. This quantity is defined in terms of the power spectral density $S_s(f) = \tilde{s}^*(f)\tilde{s}(f)$ of the Fourier transform of the time series:

$$\tilde{s}(f) = \int_{-\infty}^{\infty} e^{-2\pi i f t} s(t) dt \tag{2.57}$$

The strain amplitude spectral density is then defined as $h(f) = \sqrt{S_s(f}$. The noise power spectral density $S_n(f)$ and the signal power spectral density $S_h(f)$.ù

Noises are categorised as either a displacement noise, which directly moves the suspended mirrors causing a differential change in the arm cavity lengths, or as a sensing noise, which appears in the readout signal but is not caused by a gravitational wave.
In this paragraph are described the principal noises that dominate the limits of our sensitivity.

At lower frequencies, up to 10Hz, the main contribute to the global noise is due to vibrations of the ground which couple to the mirror motion: it shakes the optics and produces strain signals that mask gravitational wave signals.
This seismic noise could be caused by earthquakes, weather and human activity.

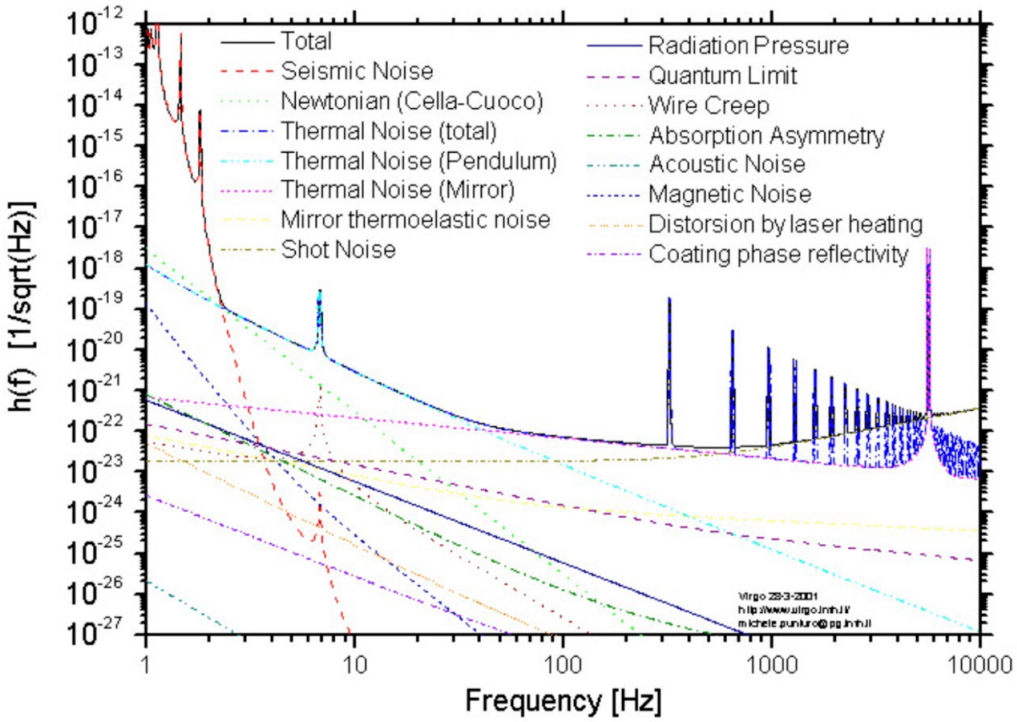

Figure 2.2. Noise budget

To reduce the potential movements of the optical elements, an attempt is made to isolate the mirrors using an advanced suspension system.

At frequencies where the seismic motion has been sufficiently reduced, between 10Hz and 500Hz, the random Brownian motion of the molecules on the surface of the mirrors and wires dominates.

The thermal energy of the interferometer's components induce vibrations both in the suspensions and in the mirrors. The nature of gravitational wave signal requires the sensitivity of the interferometric detectors to be extremely high in broad frequency band.
Therefore, the power spectrum density of the thermal noise must be considered in the development of the detectors. The Fluctuation-dissipation Theorem (FDT) relates the spectrum of the thermal noise to the amount of dissipation

$$S_n(w) = -\frac{4k_bT}{w} Im[H(w)] \tag{2.58}$$

From this equation is possible to state that the energy of fluctuations has a frequency dependent distribution; $H(z)$ is the transfer function of the system, it is a mathematical function that models the device's output, defined as

$$H(x) = \frac{1}{iWZ(w)} \tag{2.59}$$

In which $Z(w)$ is the impedance of the system in the frequency domain that can

be computed as the ratio between the Fourier components of the generalised force $\tilde{F}(w)$ and the response of the system $\tilde{X}(w)$

$$Z(w) = \frac{\tilde{F}(w)}{iw\tilde{X}(w)} \tag{2.60}$$

In the case of an harmonic oscillator, the noise spectral density is

$$S_n(w) = \frac{4k_bT}{mw} \frac{{w_0}^2\phi(w)}{(w^2 - {w_0}^2)^2 + {w_0}^4\phi^2(w)} \tag{2.61}$$

Generally, thermal noise can be reduced decreasing the dissipation with monolithic suspensions and better coatings other than lowering the temperature using criogenic payloads as it will be done in Kagra and Einstein Telescope.
Quantum mechanics limits the precision at which the test mass positions can be determined.

At high frequencies, photon shot noise limits the sensitivity, while at low frequencies it is limited by radiation pressure. The photon shot noise is produced by the natural fluctuations in the rate of photons arriving at the photodiode, that follow a Poisson process. The noise will decrease with increasing laser power, recycling cavity gain, arm cavity gain, and arm length. The corresponding noise spectral density is

$$S_n(w) = (\frac{\lambda_{laser}}{4\pi L})^2 \frac{2\hbar w_{laser}}{P} \tag{2.62}$$

Radiation pressure noise is associated with the photons from the laser striking the mirror and causing a force on the mirror. Of course, increasing the laser power to combat shot noise will actually result in an increase of radiation pressure.

$$S_n(w) = \frac{32\hbar w_{laser} P}{(4MLc\pi^2 f^2)^2} \tag{2.63}$$

This is an example of the Heisenberg's Uncertainty Principle, which says that the knowledge of the position and the momentum of a body is restricted from the relation $\delta x \delta p \geq \hbar$.
The high laser power required to determine the position of the test masses exerts a fluctuating radiation pressure which perturbs the test mass positions.
The minimun noise level is called Standard Quantum Limit (SQL) and sets a fundamental limit on the sensitivity of beam detectors, contributing to the noise as

$$S_n(w) = \frac{2\hbar}{M(\pi f L)^2} \tag{2.64}$$

Moreover, the presence of residual gas in the beam tubes would worsen the performance of the mirrors and of the laser; for this reason the vacuum system is maintained at a pressure of below 10^{-6}Pa and the noise curve of the interferometer includes only the most dominant residual gas component, hydrogen, at a pressure of 10^{-7} Pa.

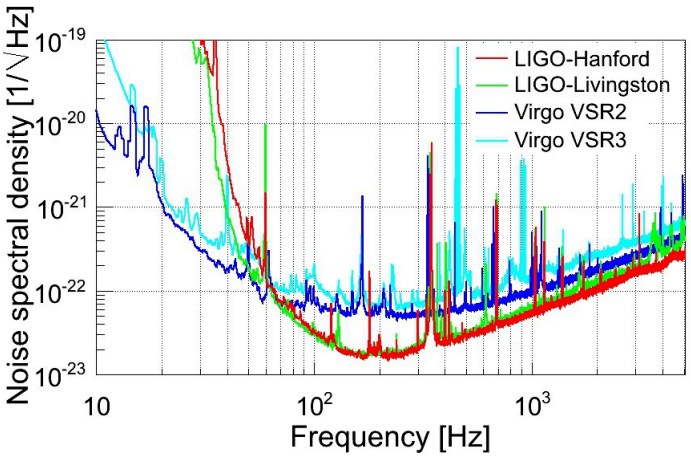

Figure 2.3. Sensitivities of the two LIGO detectors during their S6 science run, and the Virgo detector during its VSR2 and VSR3 science runs. Each curve shows the average detector noise as a function of frequency; a signal has to be significantly above the noise to be detected reliably.

2.2.3 Sources

There are four different classes of physical sources that are potential sources of gravitational waves of sufficient amplitude to be detectable by current or theorised gravitational wave detectors.

Coalescing compact binaries

Compact binary star systems, in which each member is a neutron star or black hole, are currently the best understood sources of GWs.
They are an ideal source for ground based GW detectors, as their compactness allows their orbital separation to become small enough before they merge for them to emit GWs in the detectors sensitive frequency band.
If one of the components of the binary is a neutron star then there may be an electromagnetic counterpart to the GW signal.
The loss of energy from the system will cause the orbital radius to decay, the frequency to increase, and the amplitude of the radiation to increase, producing a distinctive chirp-like signal.

Eventually, the two objects will be close enough to merge together, and the new single object will pulsate in an excite state as it tries to return to equilibrium. This phase, known as the ringdown phase, is well-modeled as a series of quasi-normal modes.
As the form of the gravitational radiation can be predicted allows a more sensitive search to be performed: knowing the form of the signal that is being search for allows powerful matched filtering techniques and signal consistency tests to be used in the attempt to detect such signals.

Bursts

A burst of gravitational waves is an event that releases a large amount of gravitational energy over a very short period of time, typically less than a few seconds.
Astrophysical events that are believed to result in a transient signal include gamma ray bursts and supernovae explosion as well as the final stages of a coalescing binary.
GW signal with a partially modelled or unknown waveform, this may be due to unknown or complicated physics, or the source may be something totally unpredicted.

The matched filtering is not a useful technique to search for this type of signal, as the waveform of a GW burst signal is unknown.
Searches for GW bursts typically search for excess power that occurs coherently between multiple detectors.
Even with no knowledge of the source of a GW signal, it is still possible to estimate some of the source parameters.
Searches for GW bursts typically give estimations of the duration, amplitude and frequency of the source. An estimation of the sky position is given by measuring the difference in arrival time between different detectors.
If the distance to the source is known, perhaps through an electromagnetic counterpart, then it is possible to estimate the energy of the source.

Continuous Sources

A periodic source is a source that emits at constant or nearly constant frequency.
The prototypical source of continuous GWs is high frequency rotating neutron stars with a non-axial deformation or low frequency binary systems composed of white dwarfs or black holes far from merger.
These sources should be present throughout the operational lifetime of a detector, so the greater the observation time, the better the sensitivity to periodic sources becomes.

Spinning neutron stars will lose energy and spin down over time, and this energy loss is due to a number of different mechanisms, including emission of gravitational radiation.
To emit a continuous GW with characteristic amplitude, a neutron star must have a non-axisymmetry in the crust. The radiation amplitude is proportional to the crucial parameter ϵ, the fractional asymmetry that is proportional to the mass of the bump on the surface.
As neutron stars emit electromagnetic radiation, it is possible to target searches of GWs for neutron stars with positions, frequencies and spin-downs known from X-ray, radio and gamma-ray observations. Examples are the Crab and Vela pulsars.

Continuous GWs have not yet been detected, but current searches have produced upper limits for their emission.
Upgraded interferometers in LIGO could set an upper limit on ϵ of order 10^{-6} for sources at ~ 10 kpc, and explain how a neutron star can be distorted to give a value of ϵ that is interesting as a GW source.
Whatever the mechanism generating the distortion, it is clear that ϵ will be small, so that $h \sim 10^{-24}$ or smaller, which is quite weak.
Measuring these waves will require coherently tracking their signal for a large number

of wave cycles, which is actually quite difficult, since the signal is strongly modulated by the Earth's rotation and orbital motion.

Searching for periodic GWs means demodulating the motion of the detector, a computationally intensive problem since the modulation is different for every sky position. Unless one knows in advance the position of the source, one needs to search over a huge number of sky position "error boxes".

Stochastic background

Stochastic backgrounds are "random" GWs, arising from a number of sources that overlap in time and frequency that are not individually resolvable.

The sum of the signals at any given time and frequency will have a random pattern that may be analyzed statistically but not predicted precisely.
A particularly interesting source of stochastic waves is the dynamics of the early Universe, which could produce an all-sky GW background, similar to the cosmic microwave background.
However, to measure waves from this epoch, we would need much more sensitive detectors than the ground-based interferometers available.

Stochastic backgrounds are usually idealized as being stationary, isotropic and homogeneous and because of their random nature they look just like noise.
Another possible background could come from astrophysical sources. These possible sources include a population of rotating neutron stars and a population of white dwarf binaries that would be important mostly for a space-based interferometers such as LISA

Chapter 3

Data analysis technique

3.1 Matched Filtering

The matched filter is the optimal linear filter technique to extract a know signal from a gaussian stochastic noise. Since the gravitational wave emission from binary coalescence is pretty well modelled, the matched filtering is the natural choice. However some complications arise: the detector background is neither stationary nor Gaussian and the knowledge of the signal is not perfect because the waveforms are approximated up to a given order and the model parameters of the incoming wave are unknown.

Consistency checks, such as the χ^2-test, are needed to discriminate true events from broadband transients of instrumental or environmental origin. To reduce the effects of the non-stationarities, vetoes can be defined to reject triggers on the base of the detector behaviour which is analysed by monitoring channels. To overcome the issues related to the unknown parameters, template banks are built covering the parameter space with a given accuracy and the filter output is computed summing in quadrature the filter outputs that involved two orthogonal-phase templates. Different approximations can be chosen to obtain waveforms as close as possible to the expected signals, with different PN orders and involving more parameters, for instance, the spin of the single components and the orbital eccentricity. Taking into account an higher number of parameters corresponds to an increment of the parameter space dimension and a growing up of the number of templates required to cover effectively the space. At the end, more templates generate more false alarms, therefore the pursuit of the best compromise between the efficiency in extracting signals and the false alarm rate is the final goal of a search.

Matched filtering technique is the standard filter choice when the expected signal is known. The technique is based on evaluating the phase-coherent correlation between the data coming from the detector and a bank of template, a copy of the model waveform weighted down by the expected power spectral density of the data, that must reproduce the expected signal. Each template of the bank is produced starting from a set of continuous waveform parameters, the amplitude, the masses $m1$, $m2$, and spins of the binary system objects and a fiducial reference time (taken to be either "time-of-arrival" t_0 or "epoch-of-coalescence" t_C) and the corresponding orbital phase ϕ_0.

The parameters describing the inclination of the binary orbit and the location of the source on the sky are degenerate with other parameters, and are therefore, ignored in the search problem, although they can be deduced once the response of three or more non-colocated detectors to a gravitational wave event is known. The eccentricity may also be ignored, since it is expected to be negligible (due to orbital circularisation) by the time the gravitational radiation enters the frequency band (10-1000 Hz) of a ground-based detector. Therefore, once the waveform equation is chosen, with a given approximation and up to a given order, the bank can be considered as a collection of points that span the parameter space.

How can a signal be taken optimally out of the noise? The assumption so far was that if a signal is present h(t) is known, then the part of the detector's output that contains the signal leads to an integral that grows, whereas integrating a single template against the noise doesn't grow as fast, it is oscillatory. However, integrating the detector output against some h(t), it is not an optimal thing because the properties of our detector are not taken into consideration.

The optimal procedure is obtaining a filter to integrate against the data knowing how the detector's output in terms of noise looks like. Instead of integrating the data against waveforms, a generic filter that is going to be integrated against the noise can be defined as:

$$s = \int_{-\infty}^{\infty} dt s(t) K(t) \tag{3.1}$$

The expectation value of s, when a signal $h(t)$ is present, is obtained simply by integrating against the probability of noise realisations

$$S =< s >_h \tag{3.2}$$

while N, the root-mean-square value when no signal is present, is defined as:

$$N = [< s^2 >_{h=0} - < s >^2_{h=0}]^{1/2} \tag{3.3}$$

3.1.1 Signal to noise ratio

The ratio S/N is by definition the signal to noise ratio, SNR, and is the expectation value of this filtering integral in the event that the signal is present, divided by its RMS value in the even no signal is present. This SNR quantity will be directly related to likelihood. The filter is going to depend from the signal and therefore, from its strength and also from the properties of the detector, and whatever the noise curve was during the data taking time. The SNR will depend on the observation time and also the length in time of signal, if one is going to be present in the detector, on the properties of the detector during the data taking time and it will depend on the kind of signal templates that one has to its disposal. The knowledge of the kind of signal that is going to be extracted is limited, if the search focuses on a signal from a CBC, it's evident that the waveform is not exactly known because the two-body problem in GR has no exact solution; the signal will be approximated to some level. The integration is not simply against some trial waveform, because some informations about the detector as well have to be combined into the research.

Given that kind of expected signal, given the kind of operating detector and the length of the data taking what choice of a filter maximises the SNR?

A more convenient form to write S and N is the Fourier domain:

$$S =< s >_h \tag{3.4}$$
$$= \int_{-\infty}^{\infty} \tag{3.5}$$
$$= \int_{-\infty}^{\infty} \tag{3.6}$$
$$= \int_{-\infty}^{\infty} \tag{3.7}$$

$$N = [< s^2 > - < s >^2]_{h=0}^{1/2} \tag{3.8}$$
$$= [< s^2 >]_{h=0}^{1/2} \tag{3.9}$$
$$= [\int_{-\infty}^{\infty} dt \int_{-\infty}^{\infty} dt\prime < n(t)n(t\prime) > K(t)K(t\prime)]^{1/2} \tag{3.10}$$
$$= [\int_{-\infty}^{\infty} df \frac{1}{2} S_n(f)|K(f)|^2]^{1/2} \tag{3.11}$$

Since the filter is just a function of time, it knows nothing about the noise, the expectation value is acting only on s(t), and this is what gets integrated against the probability density over noise realisation.

Here we have assumed that a signal is present, so s(t) is really

$$s(t) = n(t) + h(t) \tag{3.12}$$

Where n(t) is the noise but, the initial assumption is stationary gaussian noise, the expectation value of n(t) is zero. Therefore, the expectation value of s(t) is just h(t), the expected signal.

So far, we have arrived at

3.2 p-value

3.3 Template Bank

Since the parameters of an incoming gravitational wave signal will not be known a priori, the data must be searched with a set of templates, called a template bank, designed to cover the whole parameter space. The distance between the templates in the parameter space is governed by the trade-off between computational power and loss in detection rate due to the discrete nature of the template bank. The spacing should be chosen so that the loss in signal-to-noise ratio due to the mis-match of the template with the signal does not deprecate the detectability of these sources.

One can employ a geometrical approach in constructing a template bank, namely defining a metric on the parameter space and use local flatness theorem to place templates at equal distances. The template bank could be seen naively as a uniform

grid in the parameter space. Placing templates on the parameter space depends upon two crucial things: geometrical properties of the signal manifold, whether it is flat or curved, and the coordinates chosen for template placement, which could be curvilinear even when the manifold is flat, or "almost flat". Indeed, we need to choose a "Lorentzian-like" (or close to it) coordinate frame. The second point is similar to the problem of laying a regular grid on the plane using either Cartesian or polar coordinates. The situation is even more complicated because the metric, in general, depends on the waveform model and the PN order one chooses. The different PN models differ significantly from each other in their prediction of the phasing of the waves, making it necessary to search for binary black holes and neutron stars by using not one but all the different families of waveforms currently available.

The signal from a BNS sweeps through the detector bandwidth and the two neutron stars can even merge outside the sensitive bandwidth of the current ground-based detectors and the waveforms corresponding to different physical models agree reasonably well among each other (with overlaps very close to unity). For higher mass systems, e.g. BBH, the situation changes, the deviation between the various models getting more significant in the sensitive bandwidth of the detectors. Since for BBH the model waveforms from different families do not agree well with each other, a template bank that employs one PN family of templates will not be efficient to detect signals from another family. One solution is to filter the data through a number of banks with templates based on all the different models. If the reasonable assumption that at least one of the available PN models is close to the true gravitational wave signal bears out then our bank consisting of templates from all the different PN families should be efficient enough in capturing the coalescence events. Unexpectedly, we have found that the bank works well as long as the template and signal are both from the same family meaning a single template bank might suffice to filter the data through different PN families. The end result of the construction of the template bank is a set of points in the parameter space of chirptimes or, equivalently, the masses. Each point is associated with a template built from a specific signal model.

3.3.1 The lower frequency cutoff

The lower frequency cutoff f_L, which essentially determines the size of the parameter space of chirptimes and plays a crucial role in the computational resources required to process the data through the template bank. The initial fiducial frequency f_L defines the range of values of the chirptimes and is not itself a parameter to search for. However, it affects the length of the signals (therefore, the parameter space to be covered) and the SNR extracted.

3.4 Coincident and coherent research

3.5 Injections

Chapter 4

Gravitational wave observation so far

4.1 O1

4.2 O2

4.2.1 Gamma Ray Burst

4.3 O3a

Chapter 5

Black hole-neutron star binaries

5.1 Evolution of Black Hole-Neutron Star mergers

5.1.1 Tidal disruption model

5.2 Electromagnetic Counterpart of a Black Hole-Neutron Star Binary Merger

Chapter 6

My contribution to gravitational dave data analysis during O3

6.1 Bank Tests

6.2 O3 offline pyGRB analysis

6.2.1 GRB190425089

6.2.2 GRB190627A

6.2.3 GRB190728271

6.3 PyCBC O3 HL C00 data preliminary runs

6.3.1 Chunk 29

Chapter 7

Conclusions

Bibliography

[nome]